Eur. Phys. J. C (2025) 85:43
https://doi.org/10.1140/epjc/s10052-025-13750-9

THE EUROPEAN PHYSICAL JOURNAL C

Regular Article - Theoretical Physics

A perturbative approach to complexity during shearing, dissipative collapse

Kevin Reddy[1], **Megan Govender**[2,a]

[1] Department of Physics, Faculty of Applied Sciences, Durban University of Technology, Durban, South Africa
[2] Department of Mathematics, Faculty of Applied Sciences, Durban University of Technology, Durban, South Africa

Received: 9 December 2024 / Accepted: 23 December 2024

Abstract We investigate the notion of complexity as defined by Herrera et al. (Phys Rev D 97:044010, 2018) for a star undergoing dissipative collapse in the presence of shear. We adopt a perturbative scheme which tracks the onset of collapse from an initially static configuration described by the Bowers–Liang model. The complexity for the initially static configuration is driven solely by the anisotropy and grows as the difference in the radial and tangential stresses grow. As the star loses equilibrium and transits into a dissipative collapse phase, the dynamical complexity is enhanced by contributions from the anisotropy and density inhomogeneity. The novelty of our work highlights the impact of pressure anisotropy and density inhomogeneity to the evolution of the complexity factor as a self-gravitating body evolves from an initially complexity-free and static regime into a dynamical radiating stellar object in the presence of shear.

1 Introduction

The end-states of continued gravitational collapse have occupied the minds of researchers since the seminal paper by Oppenheimer and Snyder [2]. In their work, they considered the gravitational contraction of an ideal body with vanishing pressure in the interior and zero flux to the exterior spacetime. The discovery of the Vaidya solution [3] enabled researchers to model dissipative collapse in which the exterior spacetime was nonempty. The matching conditions for the smooth link up between the interior and exterior spacetimes was derived by Santos [4] for a shear-free matter distribution undergoing nonadiabatic collapse and dissipating energy in the form of a radial heat flux. Over the past three decades, the study of radiating stars has rewarded us richly with the understanding of the underlying physics such as the impact of dissipation, pressure anisotropy, shear and charge on the final outcome of the collapse process. Many of these toy models serve as a first approximation to more complicated numerical self-gravitating objects. Early models of radiative collapse incorporated pressure isotropy and the shear-free condition. The seminal work of Bowers and Liang [5] highlighted the effects of pressure anisotropy within stellar objects. They demonstrated that the inclusion of pressure anisotropy impacts on regularity, stability and causality. Herrera [6] demonstrated the instability of the pressure isotropy condition in which it was shown that an initial isotropic pressure profile will evolve into an anisotropic regime as the gravitating body leaves a state of quasi-static equilibrium. There has been an exponential increase in the number of stellar models with anisotropic pressure profiles in both the static and dynamic regimes [7–11]. There are novel approaches to incorporate anisotropy in stellar models, some of which include gravitational decoupling, shear, particle production, neutrino helicity, bulk viscosity, amongst others [12–27]. The notion of complexity within the context of stellar structure and evolution was introduced by Herrera and co-workers as early as 2010 within the context of dissipative collapse [28]. In a spherically symmetric static self-gravitating body, it was shown via a combination of scalars arising from the Riemann tensor and its contractions that the notion of complexity depends on the interplay between pressure anisotropy and density inhomogeneity [29]. The simplest system characterising vanishing complexity is one with simultaneous pressure isotropy and homogeneous density. Herrera showed that alternative scenario to vanishing complexity in nondissipative systems is when the pressure anisotropy balances out the density inhomogeneity. The condition of *vanishing complexity* leads to a quadrature which relates the two metric functions [30]. This condition has been widely exploited in the literature to construct stellar models with anisotropic pressure profile.

[a] e-mail: megandhreng@dut.ac.za (corresponding author)

Published online: 21 January 2025

Complexity in radiating stars has been studied in the literature but has mainly been restricted to shear-free collapse [31,32]. Investigations on the role of shear and its link to complexity have been presented by Herrera and his collaborators [33,34]. The difficulty in obtaining exact solutions of the Einstein field equations describing shearing, dissipative collapse is linked to solution of the boundary condition which encodes the temporal behaviour of the model. There have been various approaches to solving the boundary condition for a collapsing radiating star with a Vaidya exterior. Some of these include adhoc approaches, Lie symmetries, perturbative schemes, amongst others [35–37]. Recently, Govender et al. employed a perturbative scheme to model shear-free, dissipative collapse and addressed the evolution of complexity [38]. In this paper we extend these results to include the effects of shear via a novel approach centered on the Bowers–Liang's generalisation of the Schwarzschild uniform density sphere. This paper is structured as follows: in Sect. 2 the field equations describing the geometry and matter content for a radiating star are presented. In Sect. 3 the junction conditions required for the smooth matching ogf the interior spacetime to Vaidya's outgoing metric is given. In Sect. 4 the perturbative scheme is presented together with the perturbed equations governing the initially static configuration and the collapsing core. In Sect. 5 we introduce the static model which is described by the Bowers and Liang solution. In Sect. 6 the notion of complexity for stellar systems is revealed and we show for the first time the bifurcation of the complexity factor into static and nonstatic components. In Sect. 7 we provide an analysis of our results for a collapsing core whose precursor is described by the initially static Bower–Liang model.

2 Interior spacetime

We begin with the most general spherically symmetric line element

$$ds^2 = -A(r,t)^2dt^2 + B(r,t)^2dr^2 + Y(r,t)^2[r^2d\Omega^2], \quad (1)$$

where $d\Omega^2 = d\theta^2 + \sin^2\theta d\phi^2$ and the functions (A, B, Y) represent the potentials [39]. The matter content for the interior is described (in geometrized units) by

$$T^-_{\alpha\beta} = (\rho + P_t)V_\alpha V_\beta + P_t g_{\alpha\beta} + (P_r - P_t)\chi_\alpha\chi_\beta + q_\alpha V_\beta + q_\beta V_\alpha, \quad (2)$$

where ρ represents the energy density, P_r the radial pressure, P_t the tangential pressure and q^α the heat flux vector. The fluid four-velocity (V^α), radial unit four-vector (χ^α) and the heat flux (q^α) must satisfy the following conditions:

$$V_\alpha V^\alpha = -1, \quad \chi^\alpha\chi_\alpha = 1, \quad \chi^\alpha V_\alpha = 0 \quad , \quad V_\alpha q^\alpha = 0. \quad (3)$$

The collapse rate and the fluid four-acceleration are given by

$$\Theta = V^\alpha{}_{;\alpha}, \quad a_\alpha = V_{\alpha;\beta}V^\beta, \quad (4)$$

and the shear tensor $\sigma_{\alpha\beta}$ by

$$\sigma_{\alpha\beta} = V_{(\alpha;\beta)} + a_{(\alpha}V_{\beta)} - \frac{1}{3}\Theta(g_{\alpha\beta} + V_\alpha V_\beta). \quad (5)$$

For the comoving line element (1), the fluid four-velocity (V^α) and the radial unit four-vector (χ^α) are given respectively by:

$$V^\alpha = A^{-1}\delta^\alpha_0, \qquad \chi^\alpha = B^{-1}\delta^\alpha_1. \quad (6)$$

The heat flow vector q^α takes on the form

$$q^\alpha = (0, q_1, 0, 0) \quad (7)$$

since $V_\alpha q^\alpha = 0$ ensures radial heat flow. Using (4) with (6) yields the four-acceleration and its magnitude (scalar) in the form

$$a_1 = \frac{A'}{A}, \qquad a^\alpha a_\alpha = \left(\frac{A'}{AB}\right)^2, \quad (8)$$

and for the collapse rate we get

$$\Theta = \frac{1}{A}\left(\frac{\dot{B}}{B} + 2\frac{\dot{Y}}{Y}\right), \quad (9)$$

where dots and primes denote differentiation with respect to t and r respectively. With the aid of (5) and (6) we obtain the following nonzero components for the shear

$$\sigma_{11} = \frac{2}{3}B^2\sigma, \qquad \sigma_{22} = \sigma_{33}\sin^{-2}\theta = -\frac{1}{3}Y^2\sigma, \quad (10)$$

where

$$\sigma = \frac{1}{A}\left(\frac{\dot{B}}{B} - \frac{\dot{Y}}{Y}\right), \quad (11)$$

and the shear scalar is of the form

$$\sigma^{\alpha\beta}\sigma_{\alpha\beta} = \frac{2}{3}\sigma^2. \quad (12)$$

For a shearing, radiating matter distribution the Einstein field equations are given by

$$\rho = \frac{1}{A^2}\left(2\frac{\dot{B}}{B} + \frac{\dot{Y}}{Y}\right)\frac{\dot{Y}}{Y} - \frac{1}{B^2}\left[2\frac{Y''}{Y} + \left(\frac{Y'}{Y}\right)^2 - 2\frac{B'}{B}\frac{Y'}{Y} - \left(\frac{B}{Y}\right)^2\right], \quad (13)$$

$$p_r = -\frac{1}{A^2}\left[2\frac{\ddot{Y}}{Y} - \left(2\frac{\dot{A}}{A} - \frac{\dot{Y}}{Y}\right)\frac{\dot{Y}}{Y}\right] + \frac{1}{B^2}\left(2\frac{A'}{A} + \frac{Y'}{Y}\right)\frac{Y'}{Y} - \frac{1}{Y^2}, \quad (14)$$

$$p_t = -\frac{1}{A^2}\left[\frac{\ddot{B}}{B} + \frac{\ddot{Y}}{Y} - \frac{\dot{A}}{A}\left(\frac{\dot{B}}{B} + \frac{\dot{Y}}{Y}\right) + \frac{\dot{B}}{B}\frac{\dot{Y}}{Y}\right]$$

$$+\frac{1}{B^2}\left[\frac{A''}{A}+\frac{Y''}{Y}-\frac{A'}{A}\frac{B'}{B}+\left(\frac{A'}{A}-\frac{B'}{B}\right)\frac{Y'}{Y}\right], \tag{15}$$

$$q_1 B=\frac{2}{AB}\left(\frac{\dot{Y}'}{Y}-\frac{\dot{B}}{B}\frac{Y'}{Y}-\frac{\dot{Y}}{Y}\frac{A'}{A}\right). \tag{16}$$

In the above, ρ, p_r, p_t and q_1 are the energy density, radial pressure, tangential pressure and radial heat flux respectively.

3 Junction conditions

The exterior spacetime, which is a null atmosphere, is appropriately described by the Vaidya solution [3] which is given by

$$ds^2=-\left(1-\frac{2m(v)}{\mathscr{R}}\right)dv^2-2dvd\mathscr{R}+\mathscr{R}^2\big(d\theta^2+\sin^2\theta d\phi^2\big), \tag{17}$$

in the coordinates $x^i=(v,\mathscr{R},\theta,\phi)$, where $m(v)$ represents the Newtonian mass of the gravitating object as measured by an observer positioned at infinity.

In order to complete our model we employ the set of shearing junction conditions utilized by Reddy et al. [39] based on the pioneering work of Santos [4]. This approach does lead to a viable physical model.

The first set of junction conditions are obtained by matching the metric (1) describing the interior spacetime with the Vaidya exterior metric (17). These are given by

$$A(t,r_\Sigma)dt=\left(1-\frac{2m(v)}{\mathscr{R}_\Sigma}+2\frac{d\mathscr{R}_\Sigma}{dv}\right)^{\frac{1}{2}}dv, \tag{18}$$

$$Y(t,r_\Sigma)=\mathscr{R}_\Sigma(v). \tag{19}$$

The second set of junction conditions are obtained by matching the extrinsic curvature of the exterior spacetime to that of the interior, and are given by

$$m(v)=\left[\frac{Y}{2}\left(1+\frac{\dot{Y}^2}{A^2}-\frac{Y'^2}{B^2}\right)\right]_\Sigma, \tag{20}$$

and

$$\Big(p_r\Big)_\Sigma=\Big(q_1 B\Big)_\Sigma, \tag{21}$$

where $m(v)$ is the collective gravitational mass held within the hypersurface Σ. Substituting p_r from (28) and $\overline{q}_1 B_0$ from (41) into junction condition (22) we obtain a differential equation describing the temporal evolution of the collapse process given by

$$\alpha_\Sigma T-\ddot{T}=2\beta_\Sigma\dot{T}=\phi>0, \tag{22}$$

which holds at the boundary $r=r_\Sigma$.

Solutions that satisfy (22) include functions that are exponential as well as oscillatory. We consider an exponentially decaying function which represents an initially static system at $t=-\infty$, ie. $T(-\infty)=0$. The system is then perturbed, and undergoes exponential decay as $t\to 0$. This behaviour is ensured if $\alpha_\Sigma>0$ and $\beta_\Sigma\leq 0$. The temporal evolution of our model is then given by

$$T(t)=-T_0\exp\left[\phi t\right]. \tag{23}$$

Since the star is collapsing, we require $\dot{T}<0$.

4 Perturbative approach

We assume that the metric functions $A(t,r)$, $B(t,r)$ and $Y(t,r)$ have the same time dependence in the perturbation. The metric functions and material functions are given by

$$A(t,r)=A_0(r)+\lambda T(t)a(r), \tag{24}$$

$$B(t,r)=B_0(r)+\lambda T(t)b(r), \tag{25}$$

$$Y(t,r)=Y_0(r)+\lambda T(t)y(r), \tag{26}$$

$$\rho(t,r)=\rho_0(r)+\lambda\overline{\rho}(t,r), \tag{27}$$

$$p_r(t,r)=p_{r_0}(r)+\lambda\overline{p_r}(t,r), \tag{28}$$

$$p_t(t,r)=p_{t_0}(r)+\lambda\overline{p_t}(t,r), \tag{29}$$

$$m(t,r)=m_0(r)+\lambda\overline{m}(t,r), \tag{30}$$

$$q_1(t,r)=\lambda\overline{q}_1(t,r), \tag{31}$$

$$Y_{TF}(t,r)=Y_{TF0}(r)+\lambda\overline{Y}_{TF}(t,r), \tag{32}$$

where $0<\lambda\ll 1$, is a constant. The zero subscript is associated with the static fluid configuration and the over bar denotes the perturbed quantities.

The perturbative scheme presented here has been used by several investigators to study the evolution of collapsing stars in the presence of heat dissipation with and without shear[40–42]. Applying the perturbative framework (24)–(31) to (13)–(16) we obtain the static configuration given by

$$\rho_0=-\frac{1}{B_0^2}\left(\frac{2Y_0''}{Y_0}+\frac{Y_0'^2}{Y_0^2}-\frac{2Y_0'B_0'}{Y_0B_0}-\frac{B_0^2}{Y_0^2}\right), \tag{33}$$

$$p_{r0}=\frac{1}{B_0^2}\left(\frac{2A_0'Y_0'}{A_0Y_0}+\frac{Y_0'^2}{Y_0^2}-\frac{B_0^2}{Y_0^2}\right), \tag{34}$$

$$p_{t0}=\frac{1}{B_0^2}\left[\frac{A_0''}{A_0}+\frac{Y_0''}{Y_0}-\frac{A_0'B_0'}{A_0B_0}+\frac{Y_0'}{Y_0}\left(\frac{A_0'}{A_0}-\frac{B_0'}{B_0}\right)\right], \tag{35}$$

$$m_0=\frac{Y_0}{2}\left[1-\left(\frac{Y_0'}{B_0}\right)^2\right], \tag{36}$$

and the perturbed quantities

$$\overline{\rho}=-\frac{2bT\rho_0}{B_0}-\frac{2T}{{B_0}^2}\left[\left(\frac{y}{Y_0}\right)''-\frac{1}{Y_0}\left(\frac{b}{B_0}\right)'-\left(\frac{B_0'}{B_0}-\frac{3}{Y_0}\right)\right.$$

$$\times\left(\frac{y}{Y_0}\right)'-\left(\frac{B_0}{Y_0}\right)^2\left(\frac{b}{B_0}-\frac{y}{Y_0}\right)\Big], \tag{37}$$

$$\overline{p}_r=-\frac{2p_{r0}bT}{B_0}-\frac{2\ddot{T}y}{A_0^2Y_0}+\frac{2T}{Y_0B_0^2}\Big[Y_0'\left(\frac{a}{A_0}\right)'+\left(\frac{y}{Y_0}\right)'\times\left(Y_0'+\frac{A_0'Y_0}{A_0}\right)-\frac{B_0^2}{Y_0}\left(\frac{b}{B_0}-\frac{y}{Y_0}\right)\Big], \tag{38}$$

$$\overline{p}_t=-\frac{2bTp_{t0}}{B_0}-\frac{\ddot{T}}{A_0^2}\left(\frac{b}{B_0}+\frac{y}{Y_0}\right)+\frac{T}{B_0^2}\Big[\left(\frac{y}{Y_0}\right)''+\left(\frac{a}{A_0}\right)''+\left(\frac{2A_0'}{A_0}-\frac{B_0'}{B_0}+\frac{Y_0'}{Y_0}\right)\left(\frac{a}{A_0}\right)'-\left(\frac{A_0'}{A_0}+\frac{Y_0'}{Y_0}\right)\left(\frac{b}{B_0}\right)'+\left(\frac{A_0'}{A_0}-\frac{B_0'}{B_0}+\frac{2Y_0'}{Y_0}\right)\left(\frac{y}{Y_0}\right)'\Big], \tag{39}$$

$$\tilde{m}(r,t)=-\frac{T}{B_0^2}\left[Y_0\left(y'Y_0'-\frac{bY_0'^2}{B_0}\right)+\frac{1}{2}y\left(Y_0'^2-B_0^2\right)\right], \tag{40}$$

$$\overline{q}_1B_0=-\frac{2\dot{T}}{A_0B_0}\left[\frac{bY_0'}{B_0Y_0}+\frac{y}{Y_0}\left(\frac{A_0'}{A_0}-\frac{Y_0'}{Y_0}\right)-\left(\frac{y}{Y_0}\right)'\right], \tag{41}$$

$$\tilde{\sigma}(r,t)=\frac{\dot{T}}{A_0}\left[\frac{b}{B_0}-\frac{y}{Y_0}\right], \tag{42}$$

We can write (38) in the form

$$\overline{p}_r=-\frac{2p_{r0}bT}{B_0}+\frac{2y}{{A_0}^2Y_0}(\alpha T-\ddot{T}), \tag{43}$$

where

$$\alpha(r)=\frac{A_0^2}{yB_0^2}\Big[Y_0'\left(\frac{a}{A_0}\right)'+\left(\frac{y}{Y_0}\right)'\times\left(Y_0'+\frac{A_0'Y_0}{A_0}\right)-\frac{B_0^2}{Y_0}\left(\frac{b}{B_0}-\frac{y}{Y_0}\right)\Big]. \tag{44}$$

We can also write (41) as

$$\overline{q}_1B_0=\frac{4y\beta}{{A_0}^2Y_0}\dot{T}, \tag{45}$$

where

$$\beta(r)=\frac{A_0Y_0}{2B_0y}\Big[-\frac{bY_0'}{B_0Y_0}-\frac{y}{Y_0}\left(\frac{A_0'}{A_0}-\frac{Y_0'}{Y_0}\right)+\left(\frac{y}{Y_0}\right)'\Big]. \tag{46}$$

Substituting p_r from (28) and $\overline{q}_1B_0$ from (41) into junction condition (21) we obtain a differential equation describing the temporal evolution of the collapse process given by

$$\alpha_\Sigma T-\ddot{T}=2\beta_\Sigma\dot{T}>0, \tag{47}$$

which holds at the boundary $r=r_\Sigma$.

5 The Bowers–Liang static configuration

We take the interior static solution to be the Bowers–Liang [5] model with constant density. This model is the generalisation of the interior Schwarzschild solution to include anisotropic pressures. The Bowers and Liang model has been used extensively to investigate the role played by local anisotropy in highly dense matter distributions typically of the order of $10^{15}\,\mathrm{g\,cm^{-3}}$. If we denote the fractional anisotropy by $\Delta_f=\frac{P_t-P_r}{P_r}$ then the Bowers–Liang model exhibits the following features:

(a) $\Delta_f>0$: The maximum equilibrium mass and surface redshift are greater than their corresponding isotropic ($\Delta_f=0$) counterparts.
(b) $\Delta_f<0$: The maximum mass and surface redshift are less than their corresponding isotropic values.

Moreover, the anisotropy allows for arbitrarily large surface redshifts as observed in quasars.

The line element for the Bowers–Liang solution is

$$ds^2=-\left[\frac{3\left(1-2M/r_\Sigma\right)^{h/2}-\left(1-2m/r\right)^{h/2}}{2}\right]^{2/h}dt^2+\left(1-\frac{2m}{r}\right)^{-1}dr^2+r^2\left(d\theta^2+\sin^2\theta d\phi^2\right), \tag{48}$$

where h is a constant and $0\le r\le R$. From the metric (48) it is clear that

$$A_0^2=\left[\frac{3\left(1-2M/r_\Sigma\right)^{h/2}-\left(1-2m/r\right)^{h/2}}{2}\right]^{2/h}, \tag{49}$$

$$B_0^2=\left(1-\frac{2m}{r}\right)^{-1}, \tag{50}$$

and

$$Y_0^2=r^2. \tag{51}$$

In the physical analysis that follows we take

$$a=-k_1(r+1)^{-1},\ b=k_2(r+1)^{-1},\ y=k_3\quad\text{and}\quad m=\frac{r^3M}{R^3}, \tag{52}$$

where $k_1=k_2=10^{-17}$ and $k_3=10^{-1}$. Using (49)–(52), Eqs. (33)–(35) become, respectively,

$$\rho_o=6M/R^3, \tag{53}$$

$$p_{ro}=\left(1-\frac{2Mr^2}{R^3}\right)\times\left[\frac{4M\left(1-\frac{2Mr^2}{R^3}\right)^{\frac{h}{2}-1}}{R^3\left(3\left(1-\frac{2M}{R}\right)^{h/2}-\left(1-\frac{2Mr^2}{R^3}\right)^{h/2}\right)}-\frac{1}{r^2\left(1-\frac{2Mr^2}{R^3}\right)}+\frac{1}{r^2}\right] \tag{54}$$

$$p_{to}=\Big[6M\Big(2Mr^2\Big(-h\left(1-\frac{2M}{R}\right)^{h/2}\left(1-\frac{2Mr^2}{R^3}\right)^{h/2}-3\left(1-\frac{2M}{R}\right)^{h/2}\left(1-\frac{2Mr^2}{R^3}\right)^{h/2}+\left(1-\frac{2Mr^2}{R^3}\right)^{h}+3\left(1-\frac{2M}{R}\right)^{h}\Big)-R^3\Big(-4\left(1-\frac{2M}{R}\right)^{h/2}$$

$$\times\left(1-\frac{2Mr^2}{R^3}\right)^{h/2}+\left(1-\frac{2Mr^2}{R^3}\right)^{h}+3\left(1-\frac{2M}{R}\right)^{h}\Big)\Big)\Big]$$
$$\times\Big[R^3\left(R^3-2Mr^2\right)\Big(\Big(1-\frac{2Mr^2}{R^3}\Big)^{h/2}$$
$$-3\left(1-\frac{2M}{R}\right)^{h/2}\Big)^2\Big]^{-1} \tag{55}$$

The anisotropy parameter $\Delta = P_r - P_t$ is expressed (for the static case) as

$$\Delta=\frac{12(h-1)M^2r^2\left(1-\frac{2M}{R}\right)^{h/2}\left(1-\frac{2Mr^2}{R^3}\right)^{h/2}}{R^3\left(R^3-2Mr^2\right)\left(\left(1-\frac{2Mr^2}{R^3}\right)^{h/2}-3\left(1-\frac{2M}{R}\right)^{h/2}\right)^2} \tag{56}$$

We point out that Eqs. (57)–(58) below, including their derivation, can be found in a review article by Herrera and Santos [43]. We simply state the equations here and discuss the relationship between the order parameter Δ and the anisotropic factor C. Δ can also be written as

$$\Delta=\frac{4}{3}\pi Cr^2\Big(\rho_o+P_{ro}\Big)\Big(\rho_o+3P_{ro}\Big)\Big(1-\frac{2m}{r}\Big)^{-1} \tag{57}$$

where C, the anisotropic factor, measures the degree of anisotropy and is given by

$$h=1-2C. \tag{58}$$

It follows from Eq. (57) that the anisotropic parameter can be recast as $\Delta = C\chi(r)$, where $\chi(r)=\frac{4}{3}\pi r^2\big(\rho_o+P_{ro}\big)\big(\rho_o+3P_{ro}\big)\big(1-\frac{2m}{r}\big)^{-1}$. We also point out that $\chi(r)>0$ for all r, implying that Δ is directly proportional (and of similar sign) to C. From (58) it is clear that $h=1$ corresponds to $C=0$ which is the isotropic case, while $h=2$ and $h=4$ correspond respectively to $C=-\frac{1}{2}$ and $C=-\frac{3}{2}$ which imply that the radial pressure dominates the tangential pressure. The model has a limiting case of $h=0$ which corresponds to the Florides [44] solution which is not considered in our analysis.

6 The notion of complexity in stellar systems

The notion of complexity in stellar systems has attracted widespread attention since it was formerly introduced by Herrera and his co-workers. There have been a huge class of models of static stars based on the premise of vanishing complexity. The vanishing complexity condition within the framework of collapsing, shear-free stars was obtained by Bogadi et al. [31]. We present here the main equations governing complexity for a spherically symmetric, shearing spacetime which describes the interior of a stellar matter distribution. For a complete and insightful derivation of the following results, the reader is referred to the pioneering work of Herrera et al. [45] For the line element (1) and energy momentum tensor (2), the complexity factor for the interior spacetime can be written in terms of the metric functions as

$$Y_{TF}=\frac{1}{2A^2}\left[\frac{\ddot{Y}}{Y}-\frac{\ddot{B}}{B}-\left(\frac{\dot{Y}}{Y}-\frac{\dot{B}}{B}\right)\left(\frac{\dot{A}}{A}+\frac{\dot{Y}}{Y}\right)\right]$$
$$+\frac{1}{2B^2}\left[\frac{A''}{A}-\frac{Y''}{Y}+\left(\frac{B'}{B}+\frac{Y'}{Y}\right)\left(\frac{Y'}{Y}-\frac{A'}{A}\right)\right]$$
$$-\frac{1}{2Y^2}-\frac{\Pi}{2} \tag{59}$$

where $\Delta = \Pi = P_r - P_t$ is a measure of the pressure anisotropy. Applying the perturbative scheme (24–32) to Eq. 59 allows us to split it into static (Y_{TF0}) and time-dependent($\overline{Y}_{TF}$) components given by:

$$Y_{TF0}=\frac{{A_0}''}{A_0{B_0}^2}-\frac{{A_0}'{B_0}'}{A_0{B_0}^3}-\frac{{A_0}'{Y_0}'}{A_0{B_0}^2Y_0} \tag{60}$$

and

$$\overline{Y}_{TF}=\Bigg[\frac{a''}{A_0{B_0}^2}-\frac{a'{B_0}'}{A_0{B_0}^3}-\frac{a'{Y_0}'}{A_0{B_0}^2Y_0}-\frac{a{A_0}''}{{A_0}^2{B_0}^2}$$
$$+\frac{a{A_0}'{B_0}'}{{A_0}^2{B_0}^3}+\frac{a{A_0}'{Y_0}'}{{A_0}^2{B_0}^2Y_0}-\frac{2b{A_0}''}{A_0{B_0}^3}-\frac{{A_0}'b'}{A_0{B_0}^3}$$
$$+\frac{3b{A_0}'{B_0}'}{A_0{B_0}^4}+\frac{2b{A_0}'{Y_0}'}{A_0{B_0}^3Y_0}-\frac{{A_0}'y'}{A_0{B_0}^2Y_0}$$
$$+\frac{y{A_0}'{Y_0}'}{A_0{B_0}^2{Y_0}^2}\Bigg]T(t)+\left(\frac{y}{{A_0}^2Y_0}-\frac{b}{{A_0}^2B_0}\right)T''(t). \tag{61}$$

Using the Bowers–Liang model viz. Eqs. (49) to (51) Eqs. (60) and (61) respectively become:

$$Y_{TF0}=-\frac{12(h-1)M^2r^2\left(1-\frac{2M}{R}\right)^{h/2}\left(1-\frac{2Mr^2}{R^3}\right)^{h/2}}{R^3\left(R^3-2Mr^2\right)\left(\left(1-\frac{2Mr^2}{R^3}\right)^{h/2}-3\left(1-\frac{2M}{R}\right)^{h/2}\right)^2} \tag{62}$$

and

7 Physics of the model

We now turn our attention to the physical viability of the model. Starting off with the initial static configuration, we note that for the Bowers–Liang model, the density is constant and describes a uniform density sphere with anisotropic pressure for $h \neq 1$. The radial pressure as a function of the radial coordinate is plotted in Fig. 1. We observe that the radial pressure is a monotonically decreasing function of the radial coordinate and vanishes for some finite $r = r_b$, which defines the boundary of the star. We further note that the

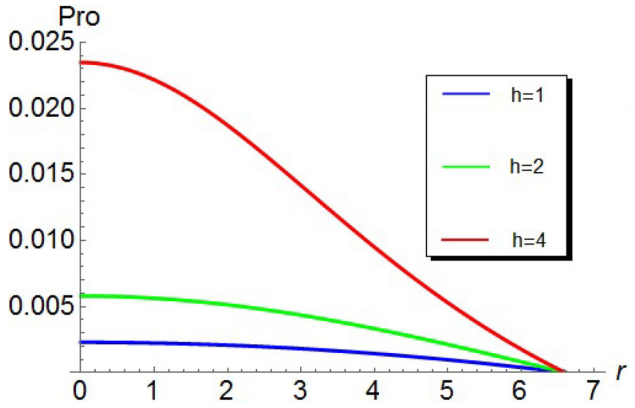

Fig. 1 Static radial pressure, P_{ro}. $M = 1$, $R = 6.6$

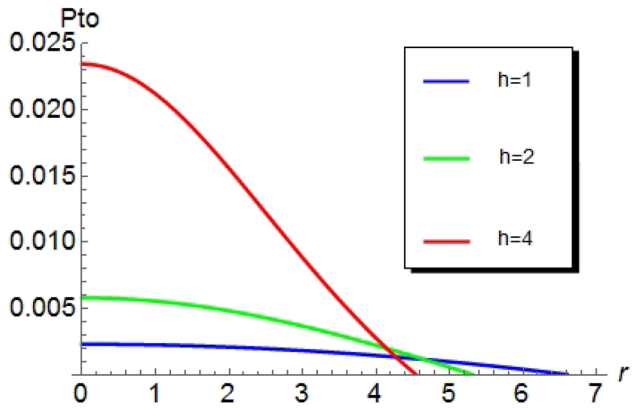

Fig. 2 Static tangential pressure, p_{to}. $M = 1$, $R = 6.6$

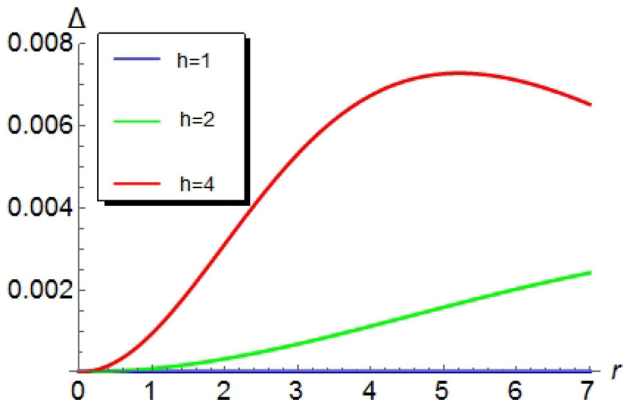

Fig. 3 Static pressure anisotropy $\Delta = P_{ro} - P_{to}$. $M = 1$, $R = 6.6$

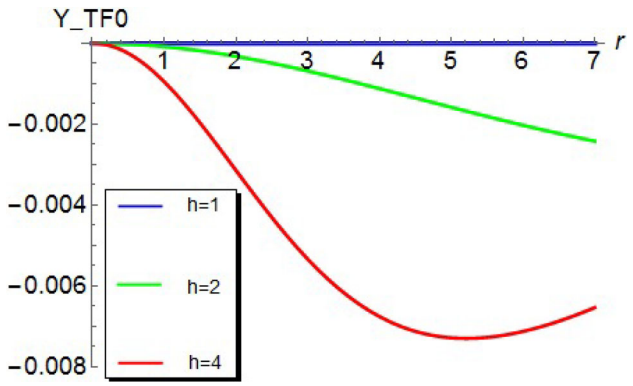

Fig. 4 Static complexity, Y_{TF0}. $M = 1$, $R = 6.6$

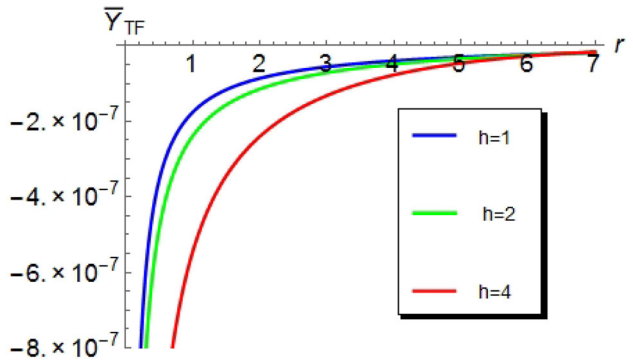

Fig. 5 Perturbed complexity $\overline{Y}_{TF}$ for early time, $M = 1$, $R = 6.6$, $t = -100$, $\phi = 0.01$

radial pressure increases at each interior point of the stellar configuration as the anisotropy parameter, h is increased. The tangential pressure is displayed in Fig. 2. The tangential stresses are everywhere positive and decreases monotonically towards the surface layers of the star. It is interesting to note that the tangential pressure vanishes at some $r = r_0$, which decreases as h increases, i.e., the magnitude of the anisotropy determines where the tangential stress has no influence on the star. The anisotropy factor is displayed in Fig. 3. Anisotropy increases with an increase in h with the isotropic case given by $h = 1$. Furthermore, $\Delta > 0$ everywhere inside the star signifying an inwardly directed force due to anisotropy. This attractive force couples with the inwardly driven gravitational interaction thus providing a mechanism for loss of hydrostatic equilibrium.

Figure 4 indicates that the complexity factor for the initially static Bowers–Liang configuration is everywhere negative. Comparing Figs. 3 and 4 we observe that magnitudes of Δ_0 and Y_{TF0} are equal in magnitude, that is to say that for this model, the complexity is driven by the anisotropy as there are no contributions from density inhomogeneity. As expected that complexity vanishes when $h = 1$ and grows in magnitude with increasing h. In Figs. 5 and 6, we have plotted the perturbations of the complexity factor for early and late time collapse. The gradient of these perturbations closer to the center of the star are is larger than +its counterpart in the surface layers. The perturbations vanish towards the stellar surface. For late times, we note that the perturbations of the complexity factor 'ease' off, i.e., the gradient of the complexity profile decreases as compared to early time collapse. The late time perturbations die off at the stellar surface. In Figs. 5 and 6, we have plotted the perturbations of the complexity factor for early and late times, respectively.

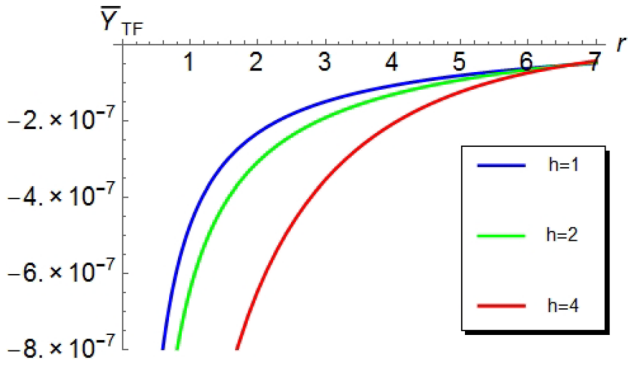

Fig. 6 Perturbed complexity $\overline{Y}_{TF}$ for late time, $M = 1$, $R = 6.6$, $t = -1$, $\phi = 0.01$

While the magnitude of the perturbations are of the same order for the different epochs of the collapse, we note that the spatial gradient of the complexity factor is higher in the central regions of the collapsing body for early times. This could be attributed to the production of heat energy close to the center of the star. The perturbations attributed to complexity attenuate rapidly in the surface layers for early times. We can understand this by noting that for late times heat is carried away from the central regions towards the surface of the star more efficiently.

8 Conclusion

In this work, we provided a general perturbative framework which addresses the notion of complexity in stars undergoing dissipative collapse in the form of a radial heat flux and in the presence of shear. The collapse proceeded from an initially static configuration described by the Bowers–Liang model which has an associated 'switch' which controls the degree of anisotropy. Since the Bowers–Liang model describes an anisotropic, uniform density sphere, the complexity is driven solely by pressure anisotropy. As the star loses hydrostatic equilibrium and begins to radiate, the complexity is governed by anisotropy, density inhomogeneity and heat flux. We showed that the perturbations to the complexity factor are behave substantially different for different epochs of the collapse process as well as in different regions of the collapsing body. We believe that our work sheds new light on complexity in radiating systems and has highlighted the need for more general matter distributions.

Acknowledgements MG acknowledges financial support from the National Research Foundation under Grant number 146050.

Data Availability Statement This manuscript has no associated data or the data will not be deposited. (Authors' comment: All data was obtained using the formulae explicitly given in the article.)

Code Availability Statement The manuscript has no associated code/software. [Author's comment: Code/Software sharing not applicable to this article as no code/software was generated or analysed during the current study.]

Funded by SCOAP[3].

References

1. L. Herrera, Phys. Rev. D **97**, 044010 (2018)
2. J.R. Oppenheimer, H. Snyder, Phys. Rev. **56**, 455 (1939)
3. P.C. Vaidya, Proc. Indian Acad. Sci. A **33**, 264 (1951)
4. N.O. Santos, MNRAS **216**, 403–410 (1985)
5. R.L. Bowers, E.P.T. Liang, Astrophys. J. **188**, 657 (1974)
6. L. Herrera, Phys. Rev. D **101**, 104024 (2020)
7. L. Herrera, J. Ospino, A. Di Prisco, Phys. Rev. D **77**, 027502 (2008)
8. S.A. Ngubelanga, S.D. Maharaj, Eur. Phys. J. Plus **130**, 211 (2015)
9. N.F. Naidu, M. Govender, S.D. Maharaj, Eur. Phys. J. C **78**, 48 (2018)
10. M. Govender, A. Maharaj, K.N. Singh, N. Pant, Mod. Phys. Lett. A **10**, 1142 (2020)
11. S.C. Jaryal, Eur. Phys. J. C **80**, 683 (2020)
12. J. Ovalle, Phys. Rev. D **95**, 104019 (2017)
13. J. Ovalle, Mod. Phys. Lett. A **23**, 3247 (2008)
14. J. Ovalle, F. Linares, Phys. Rev. D **88**, 104026 (2013)
15. G. Abellán, Á. Rincón, E. Fuenmayor, E. Contreras, Eur. Phys. J. Plus **135**(7), 606 (2020)
16. S.K. Maurya, R. Nag, Eur. Phys. J. C **82**, 48 (2022)
17. S.K. Maurya, M. Govender, S. Kaur, R. Nag, Eur. Phys. J. C **82**, 100 (2022)
18. C. Arias, E. Contreras, E. Fuenmayor, A. Ramos, Ann. Phys. **436**, 168671 (2022)
19. J. Andrade, E. Contreras, Eur. Phys. J. C **81**, 889 (2021)
20. M. Carrasco-Hidalgo, E. Contreras, Eur. Phys. J. C **81**, 757 (2021)
21. R. Casadio, E. Contreras, J. Ovalle, A. Sotomayor, Z. Stuchlik, Eur. Phys. J. C **79**, 826 (2019)
22. S.K. Maurya, A. Errehymy, R. Nag, M. Daoud, Fortschr. Phys. **70**, 2200041 (2022)
23. S.K. Maurya, F. Tello-Ortiz, M. Govender, Fortschr. Phys. **69**, 2100099 (2021)
24. S.K. Maurya, K.N. Singh, M. Govender, S. Hansraj, Astrophys. J. **925**, 208 (2022)
25. S.K. Maurya, M. Govender, K.N. Singh, R. Nag, Eur. Phys. J. C **82**, 49 (2022)
26. J. Martinez, Phys. Rev. D **53**, 6921 (1996)
27. J.M.Z. Pretel, M.F.A. Da Silva, MNRAS **495**, 5027–5039 (2020)
28. L. Herrera, A. Di Prisco, J. Ospino, Gen. Relativ. Gravit. **42**, 1585 (2010)
29. L. Herrera, Phys. Rev. D **97**, 044010 (2018)
30. R. Casadio, E. Contreras, J. Ovalle, A. Sotomayor, Z. Stuchlík, Eur. Phys. J. C **79**, 826 (2019)

31. R.S. Bogadi, M. Govender, Eur. Phys. J. C **82**, 475 (2022)
32. R.S. Bogadi, M. Govender, S. Moyo, Eur. Phys. J. C **82**, 747 (2022)
33. L. Herrera, A. Di Prisco, Phys. Rev. D **109**, 064071 (2024)
34. L. Herrera, A. Di Prisco, J. Ospino, Symmetry **16**, 341 (2024)
35. S.M. Wagh, M. Govender, K.S. Govinder, S.D. Maharaj, P.S. Muktibodh, M. Moodley, Class. Quantum Gravity **18**, 2147 (2001)
36. A. Paliathanasis, M. Govender, G. Leon, Eur. Phys. J. C **81**, 718 (2021)
37. S.D. Maharaj, N. Naidoo, G. Amery, K.S. Govinder, Eur. Phys. J. C **83**, 333 (2023)
38. M. Govender, R.S. Bogadi, W. Govender, N. Mewalal, Astrophys. Space Sci. **369**, 25 (2024)
39. M. Govender, K.P. Reddy, S.D. Maharaj, IJMP-D **23**, 1450013 (2014)
40. L. Herrera, N.O. Santos, Phys. Rep. **286**, 53 (1997)
41. M. Govender, K.P. Reddy, W. Govender, S.D. Maharaj, Eur. Phys. J. C **81**, 177 (2021)
42. N.F. Naidu, R.S. Bogadi, A. Kaisavelu, M. Govender, Gen. Relativ. Gravit. **52**, 79 (2020)
43. L. Herrera, N.O. Santos, Phys. Rep. **286**, 53 (1997)
44. P.S. Florides, Proc. R. Soc. Lond. A **337**, 529 (1974)
45. L. Herrera, A. Di Prisco, J. Ospino, Phys. Rev. D **98**, 104059 (2018)